Journal of Sustainable Development of Energy, Water and Environment Systems

http://www.sdewes.org/jsdewes

Year 2026, Volume 14, Issue 4, 114074,

Original Research Article

AI-Driven Forecasting of Hydrogen and Aluminium Hydroxide Production from Aluminium Slag in Saudi Arabia

Rami I. Al Najada* [*1], Mohamed Mahmoud[2,3], Mian M. Shaukat1[1]

[1]Department of Mechanical Engineering
King Fahd University of Petroleum and Minerals
e-mail: g202391690@kfupm.edu.sa, mshaukat@kfupm.edu.sa

[2]Department of Civil and Environmental Engineering
Polytechnic University of Milan
e-mail: Mohamed.mahmoud@polimi.it

[3]Department of Construction Engineering
Misr University of Science and Technology
e-mail: mohamed.ashraf@must.edu.eg

Cite as: Al Najada, R., Mahmoud, M., Shaukat, M. M., AI-Driven Forecasting of Hydrogen and Aluminium Hydroxide Production from Aluminium Slag in Saudi Arabia, J.sustain. dev. energy water environ. syst., 1140743, 2026, DOI: https://doi.org/10.13044/j.sdewes.d14.0743

ABSTRACT

The fast development of aluminium production in Saudi Arabia has led to proportionally increased amounts of industrial waste that present both environmental risks and potential chances for resource recovery. The hydrolysis of waste aluminium slag through seawater to create green hydrogen along with aluminium hydroxide is presented in this work as a potential to improve waste management through the conversion of aluminium waste into marketable products, thereby reducing greenhouse gas emissions and creating financial opportunities that promote sustainable resource management and green energy solutions, supporting the kingdom's Vision 2030 energy transition plans. This case study utilises the XGBoost machine learning algorithm to forecast aluminium production growth in Saudi Arabia and estimate future aluminium slag availability and the production of hydrogen and aluminium hydroxide. Economic growth and industrial demand served as the basis for these estimates. The model achieved a Mean Absolute Percentage Error of 6.9%, and analysis shows that aluminium production is projected to increase from 784.88 Kilotonnes in 2025 to 1,058.42 Kilotonnes in 2041, with slag generation rising from 156.98 to 211.68 Kilotonnes and enabling up to 6.83 million kilograms of green hydrogen and 176.2 Kilotonnes of aluminium hydroxide annually by 2041. The economic analysis indicated that the process relies strongly on the dual-value stream generated by hydrogen and aluminium hydroxide, supporting the commercial attractiveness of aluminium slag valorisation. The economic viability, carbon mitigation advantages, and industrial growth potential outcomes of this approach contribute to sustainable energy research by integrating AI-driven forecasting with circular waste-to-hydrogen valorisation for decarbonising the aluminium sector in the region.

KEYWORDS

Green hydrogen, Waste-to-energy optimization, Machine learning, XGBoost, Circular economy, Sustainable Development Goals, Recycling

* Corresponding author

INTRODUCTION

Waste-to-energy (WtE) systems remain vital components of sustainable development, addressing both energy shortages and waste management issues. The conversion of industrial waste together with municipal waste and agricultural waste produces energy in forms such as electricity, heat, and fuel products [1]. Existing WtE conversion technologies, which include anaerobic digestion, pyrolysis, and gasification, have proven their ability to decrease environmental problems while creating economic benefits [2]. The WtE operation exists today as a circular economy approach where industrial waste serves simultaneously as a source of sustainable energy and material extraction for clean products [3].

The production of green hydrogen from waste resources has established itself as an appealing solution within this expanding field [4]. Hydrogen plays an essential role in power generation, manufacturing, and transport applications through its clean energy functions as a carrier. Traditional hydrogen production through steam methane reforming emits a significant carbon footprint while requiring large quantities of water [5]. Thus, researchers have explored numerous pathways for more sustainable hydrogen process routes [6]. Researchers are exploring treating waste as valuable precursors for hydrogen production [7], such as biomass and organic solid waste [8]. The generation of hydrogen through metal hydrolysis and other scalable chemical reactions using aluminium-rich industrial waste, including aluminium slag, provides an environmentally friendly and economically viable solution [9]. This process demonstrates both waste reduction and emission mitigation benefits and shows rising cost competitiveness where production costs reach competitive values [10].

Studies from recent literature confirm that aluminium-seawater [11] and salt-promoted aluminium-water reactions [12] demonstrate feasible technological implementation [13], and environmental sustainability benefits for hydrogen production processes [14]. This effect is also seen in the hydrolysis of magnesium to produce hydrogen [15]. The aluminium-seawater hydrolysis process delivers high hydrogen production along with minimal carbon emissions and generates valuable aluminium-based by-products, which make it appealing both environmentally and commercially [16]. However, given the oxidation nature of metallic aluminium, activation methods must take place to promote efficient reaction kinetics [17]. As seen in [11], the presence of Sodium Chloride (NaCl) in various concentrations as artificial seawater significantly increased the reaction rates of liquid metal-activated aluminium plates to produce hydrogen. Optimising and scaling such systems requires accurate production level forecasts and resource availability predictions, as industrial waste generation and market demand show high variability.

Recent studies demonstrate hydrogen production from aluminium slag/dross via hydrolysis with seawater or alkaline solutions, yielding 0.71 L H_2/g Al in NaCl-activated reactions at 20°C [18], up to 1.2 L/g theoretically from metallic Al content (15-30%) [19], and comparable rates to pure Al after milling activation[20]. Aluminium hydroxide ($Al(OH)_3$) emerges as a byproduct via $2Al + 6H_2O \rightarrow 3H_2 + 2Al(OH)_3$, with near-100% purity post-reaction [21]. However, limitations include oxide passivation requiring mechanical/Ga-In activation [22], $Al(OH)_3$ aggregation restricting water access, and variable metallic Al recovery [21]. Machine learning (ML) aids prediction: Artificial Neural Networks (ANN) modelled H_2 yields from Al-Sodium hydroxide (NaOH) reactions [19], XGBoost excelled in steel/energy forecasting ($R^2 > 0.97$) [23], and gradient boosting predicted dark fermentation H_2 under data scarcity [24], but Saudi-specific slag forecasting remains unexplored.

The eXtreme Gradient Boosting (XGBoost) algorithm, along with other ML tools, serves as a powerful system for predictive modelling and proactive planning, as well as system

optimisation in this context [25]. The XGBoost algorithm effectively processes structured data, providing high accuracy and scalability through its extreme gradient-boosting mechanisms based on decision trees [26]. The system develops sequential weak prediction models, mostly consisting of decision trees, through a process that optimises a loss function via gradient descent optimisation. XGBoost can demonstrate effectiveness in waste-to-energy modelling as it can detect sophisticated nonlinear patterns between economic indicators and industrial output with material properties together with target variables, including hydrogen and $Al(OH)_3$ yields [27]. Through its analysis of past and current data, XGBoost makes accurate predictions about future output, enabling the design of efficient systems while planning facility investments ahead of time.

Researchers in literature utilised XGBoost to make various predictions. These fields can include predictive maintenance [28], housing prices [29], and optimising water electrolysis [30] and other hydrogen production methods [31], as well as predicting the performance of hydrogen production reactions [32]. Researchers studied how XGBoost could be used to forecast electricity consumption [33]. The method effectively deals with diverse influencing variables as well as user behavioural patterns that affect regional power consumption predictions. XGBoost serves to develop prediction models for various user groups, which validates its capability to predict short-term power consumption. Research about XGBoost forecasting aluminium mining output does not exist in Saudi Arabia yet, but it has shown successful results (Root Mean Square Error (RMSE) / Mean Absolute Percentage Error (MAPE) reductions >25%) in related sectors like mining revenues [34] and energy demand [35]. Recently, researchers explored utilising statistical tools or ML methods, considering Saudi government economic factors for industrial energy and decarbonisation [36]. Researchers are currently examining metal slag composition before production ends, rather than predicting it post-production, which could solve a major problem in waste prevention planning [37].

Traditional methods for predicting aluminium production, such as linear regression and time-series analysis, often struggle to capture the complex interplay of variables influencing mining activities [38]. ML models, renowned for their ability to discern nonlinear patterns in multidimensional datasets [39], offer a promising alternative [40]. Among ML algorithms, XGBoost has emerged as a preeminent tool for industrial forecasting due to its computational efficiency, robustness to overfitting, and capacity to handle heterogeneous data types from macroeconomic indicators to real-time operational metrics. While chemical engineering simulations such as computational fluid dynamics (CFD) and process flowsheeting provide mechanistic fidelity for reactor-scale hydrolysis kinetics and multiphase transport [41], they presuppose exhaustive physicochemical parameters often unavailable for prospective waste streams like variable Saudi slag compositions (15-25% yield range) and may falter in extrapolating macroeconomic drivers that dominate long-term yield forecasting [42].

The rapid growth of aluminium production across Saudi Arabia makes this forecasting method suitable for predicting the scale of the expanding aluminium slag output. The Saudi Vision 2030 serves as the catalyst for national efforts involving sustainable technologies that both decrease environmental impact and increase energy security. The future success and scalability of such systems depend on accurate predictions of upcoming trends, along with the implementation of suitable infrastructure beforehand. Herein, employ XGBoost for upstream aluminium production prediction, where the model will be trained on Maaden's (Saudi Arabian Mining Company) data between 2005 and 2023. . The primary objectives of this work are threefold: (1) to develop an XGBoost model capable of predicting annual aluminium production in Saudi Arabia with high temporal resolution and accuracy; (2) to establish a

deterministic framework for translating predicted production volumes into slag generation estimates using empirically derived conversion ratios; and (3) to validate the model's outputs against historical production data and experimental slag measurements, thereby quantifying its utility for industrial and environmental planning.

METHODS

The study evaluates the feasibility of implementing a batch reactor for aluminium dross hydrolysis to generate hydrogen and $Al(OH)_3$. The method requires three basic elements: waste aluminium slag (dross), NaOH and seawater. The process generates three main output components: green hydrogen, $Al(OH)_3$, and thermal energy. Post-industrial aluminium dross, which originates from aluminium ore smelting refineries, serves as the aluminium feedstock for this study. Dross is a significant waste component of the aluminium melting process [43].

Reaction Characteristics

The quantity of aluminium mining and production in Saudi Arabia was obtained from Ma'aden's annual reports on mining [44]. Furthermore, the aluminium slag, or dross generation rate, was estimated from literature based on recent production technologies. The yearly amount of aluminium slag was established based on the percentage value of Ma'aden's annual production reports in metric tons, which became a key factor for yield projection. For this work, it is assumed that for 1000kg of aluminium produced by the factory, a corresponding 20% is generated [45]. Other works have estimated that dross generation ranges from 8% black dross per tonne of molten metal produced [46], and up to 15%. [47].

Research shows that the metallic aluminium composition in the dross can significantly vary between samples [48], and could reach up to 50% of the composition of black dross [46]. In this work, the metallic aluminium available in the dross is set to 30% to mitigate overemphasis on material production results and account for losses in the process line. The initial reaction in the reactor is the aluminium reacting with water in the presence of NaOH to form sodium aluminate ($NaAl(OH)_4$), which further breaks down to NaOH again and $Al(OH)_3$. The maximum available hydrogen production from aluminium hydrolysis is obtained by stoichiometry of the following reaction:

$$2Al + 6H_2O \rightarrow 3H_2 + 2Al(OH)_3 \quad (1)$$

To obtain the Gibbs free energy for the reaction (ΔG_{rxn}), and standard reaction enthalpy (ΔH_{rxn}):

$$\Delta G_{rxn} = \left(2 \cdot g_{Al(OH)_3} + 3 \cdot g_{H_2}\right) - \left(2 \cdot g_{Al} + 6 \cdot g_{H_2O}\right) \quad (2)$$

$$\Delta H_{rxn} = \left(2 \cdot h_{Al(OH)_3} + 3 \cdot h_{H_2}\right) - \left(2 \cdot h_{Al} + 6 \cdot h_{H_2O}\right) \quad (3)$$

Calculating the Gibbs free energy and the reaction enthalpy at 100°C from The National Institute of Standards and Technology (NIST) [49] data yields -285 kJ/mol H2, and -284 kJ/mol H_2, respectively. This indicates a spontaneous, highly exothermic reaction. The addition of

NaOH in the reaction can be expressed in the reaction below, to form hydrogen gas and $NaAl(OH)_4$:

$$2Al + 2NaOH + 6H_2O \rightarrow +2NaAl(OH)_4 + 3H_2 \quad (4)$$

The $NaAl(OH)_4$, solution can be further broken down to regenerate NaOH, for instance, by the crystallisation of $2Al(OH)_3$ [50]:

$$2NaAl(OH)_4\,(aq) \rightarrow 2Al(OH)_3\,(s) + 2NaOH\,(aq) \quad (5)$$

The molar ratio for producing hydrogen is 3:2, where 3 moles of hydrogen are produced for every 2 moles of aluminium reacted. For $Al(OH)_3$, the ratio is 1:1. The nature of this reaction is exothermic. Therefore, no heating will be provided to the system as it is expected to be catalysed by its own thermal energy production.

Seawater acts as the medium for conducting hydrolysis reactions. The study assumes seawater will be collected from coastal regions or rejected brine streams in desalination plants, as these sources contain high salinity content with little economic utilisation. By employing seawater as a reaction medium, the production process becomes more environmentally sustainable, as it avoids the use of freshwater while still meeting sustainable water usage requirements. Employing reject brine may be feasible in this case study, as the Ras Al Khair Industrial City in the Saudi Arabian Eastern Region houses both one of the world's largest aluminium production facilities and a desalination plant. Figure 1 showcases the reactor process diagram.

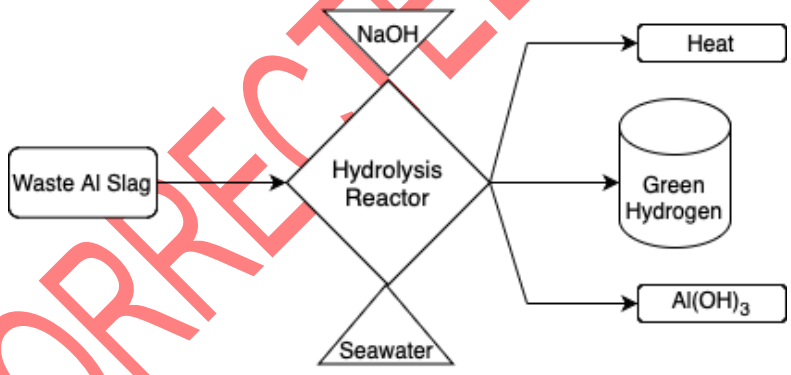

Figure 1. Reactor Process Diagram

The addition of NaOH serves as a catalyst, increasing aluminium slag reactivity during hydrolysis by removing surface oxide layers that protect aluminium components in bulk dross. The industrial chemical suppliers located within the Gulf region provided NaOH prices in bulk amounts. This analysis incorporates typical commercial procurement processes, including delivery to the reaction location.

A stainless-steel batch reactor served as the model for hydrolysis, as it demonstrates both chemical compatibility and high-salinity resistance. A similar batch reactor has been experimented with in literature for aluminium-based processes for hydrogen production [51], as well as other experiments with aluminium/seawater reactions [52], including artificial seawater [53]. The commercial vendor supplied specifications for the reactor type, which served as the basis for manufacturer-provided cost quotations. The reactor contains this specific design to manage efficient thermal regulation alongside manageable batch processing. The parameters of the reactor system determined capital expenditure costs and input data for

simulating hydrogen and $Al(OH)_3$ output quantities. However, it should be noted that research conducted by the authors revealed some patents; however, no such apparatus has been observed in commercial use.

Hydrogen and $Al(OH)_3$ quantities are initially estimated on a stoichiometric upper-bound basis using the balanced hydrolysis reaction. Actual conversion rates would be lower due to factors such as dross heterogeneity, oxide-layer passivation, mixing and mass-transfer limitations, and separation losses. Hydrogen production values represent the gross H_2 generated at the reactor outlet; the final purity depends on gas conditioning, which includes removal of moisture and particulates, and is considered an implementation consideration here. The hydrolysis reaction is exothermic and can provide low-grade thermal energy that can be recovered through heat integration [54]; however, the proportion of recoverable heat depends on the design, and thermal recovery is not included in the baseline economic analysis to ensure a conservative estimate.

Machine Learning Approach to Forecasting Aluminium Mining in Saudi Arabia

XGBoost is a tree-based ensemble ML approach that uses gradient boosting methods to achieve its purpose. The procedure creates multiple basic tree models using decision trees, which minimise prediction errors by performing gradient descent on specified loss functions sequentially [25]. Numerous users appreciate XGBoost because it provides scalable solutions that produce efficient computations to discover complex nonlinear connections in orderly datasets. Its capabilities match exactly the requirements of industrial forecasting because it detects production output changes influenced by several economic, environmental, and operational elements. XGBoost enables the modelling of multifactorial aluminium mining systems beyond traditional stationarity constraints because it does not require maintaining statistical consistency between different time intervals, and it accommodates both time-invariant and time-variant feature characteristics [55]. The deployment of XGBoost in this study is also seen in Figure 2.

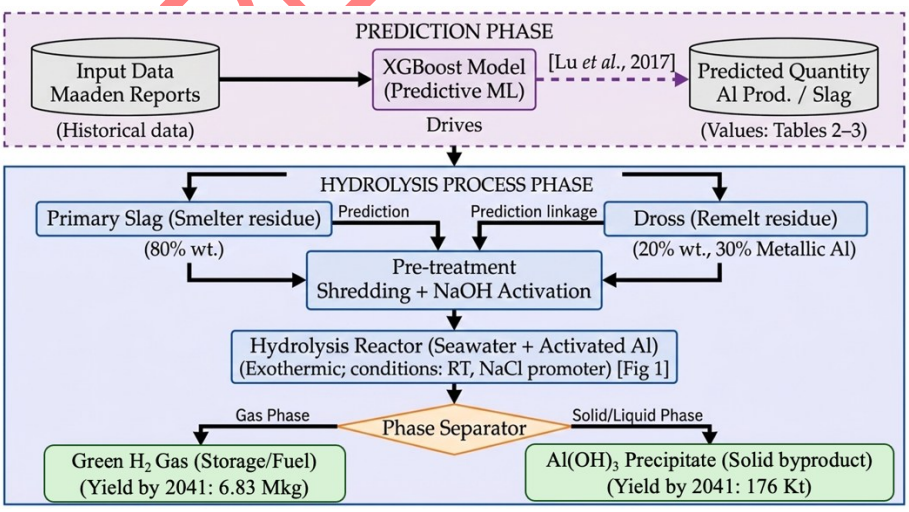

Figure 2. Detailed chemical reaction phases and the role of XGBoost prediction phase

Maaden's data were used, with training spanning from 2005 to 2018 and testing from 2019 to 2023. The model achieved a MAPE of 6.9%, due to its empirical advantages such as superior nonlinear inference from sparse, heterogeneous features, including 15 inputs like lagged Gross Domestic Product (GDP) and policy binaries, compared to linear autoregressive baselines. In addition, it demonstrated robustness to small datasets through L1/L2 regularisation and early

stopping after 10 epochs on Mean Squared Error (MSE). Additionally, the approach proved to be computationally efficient, taking seconds to run 500 estimators versus weeks with CFD. This data-centric paradigm outperforms pure simulations for strategic planning horizons (2041 slag: 211 kilotons (Kt)), enabling Monte Carlo uncertainty propagation (95% Confidence Interval (CI) 14.5%) absent in parameter-heavy models, though future SHapley Additive exPlanations (SHAP) interpretability and CFD fusion could refine micro-kinetics. [56].

Data acquisition and preprocessing. The research relies on a systematic approach to acquire and enhance data from multiple sources to establish reliable predictive modelling foundations [57]. The research activities focused on discovering multiple elements that affect aluminium production in Saudi Arabia through economic analysis and operational and policy examinations. Ma'aden's annual reports from 2005 to 2023 provided detailed statistics about primary production, including annual aluminium output and efficiency rates and regional operational measurements. National industrial bulletins issued by the Saudi Ministry of Energy delivered information about Vision 2030 resource distribution along with production capacity updates. GDP growth figures, along with industrial sector data and energy price statistics, were acquired from Ma'aden's report. The full details of the ML methodology in this study can be observed in Figure 3 and the supplementary information document.

Estimating aluminium slag generation using predictive outputs. The calculation of aluminium slag output relies on proven empirical conversion factors that explain the connection between aluminium production and byproduct slag quantities. The smelting methods used in Gulf Cooperation Council (GCC) nations produce primary aluminium slag, which accounts for 15–25% of the total manufacturing mass. The specified range illustrates variations between different smelting methods and raw material quality levels, as well as operational performance standards. The slag yield from high-purity alumina smelters in Saudi Arabia runs between 18% and 22% based on metallurgical analysis of slag composition, according to Ma'aden management data. Expert analysis showed that slag contains primarily metallic aluminium (12–18%) and aluminium oxide (50–65%) with minimal nitrides and carbides, in addition to small adjustments that result from furnace settings and alloy formation. The analysis established a specific conversion rate of 20% for accurate and actionable predictions that match the highest recorded values found in Resources, Conservation & Recycling, and validate Ma'aden's historical data from 2015 through 2023. The ratio utilises real-world findings to combine technical accuracy with practical considerations [58], managing natural process variations to establish a solid foundation for waste management strategy development [59].

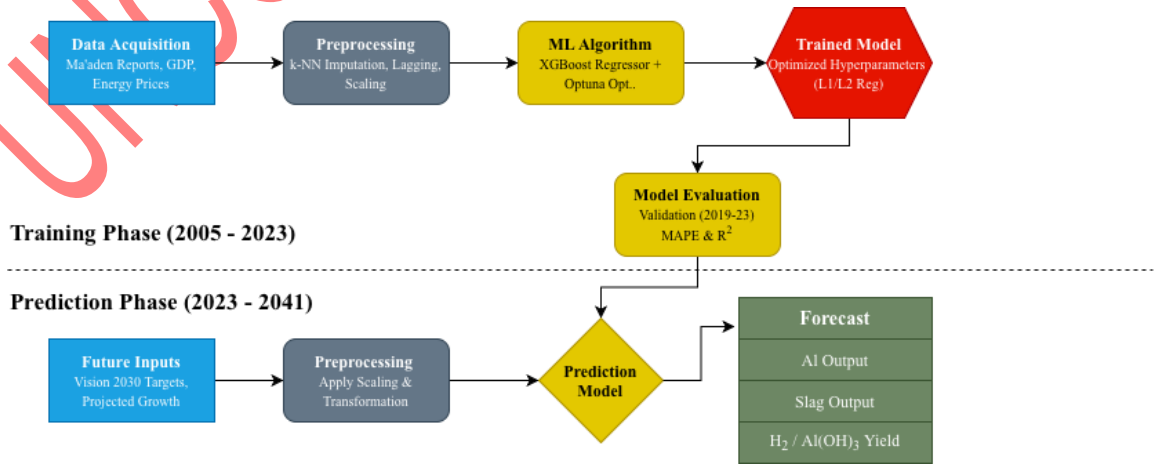

Figure 3. The ML process employed in this work

RESULTS

The XGBoost regression model used for aluminium production prediction, and as seen in Figure 4, goes through steady annual output expansion. The projected production figures reveal sales will expand from 784.88 Kt to 1,058.42 Kt throughout the forecast duration (2025–2041) with a 34.8% growth rate at 1.9% in Compound Annual Growth Rate (CAGR) (Table 1). The model generated small 95% confidence interval ranges, which expanded minimally from ±7.3% in 2025 to ±5.6% during 2041.

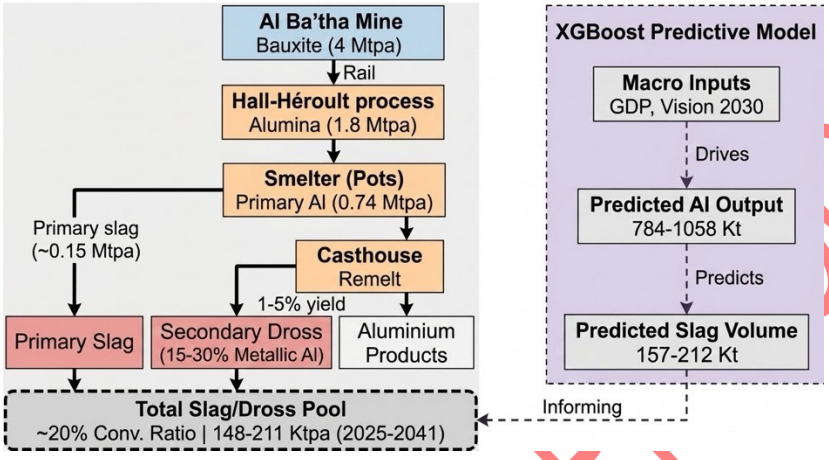

Figure 4. Integrated aluminium value-chain and modelling workflow used in this study

Table 1. Forecasted Aluminium Production and Annual Growth Rates (2025–2041)

Year	Predicted Production (Kt)	Lower Bound (Kt)	Upper Bound (Kt)	Annual Growth Rate (%)
2025	784.88	727.83	841.75	–
2026	807.24	751.27	865.46	2.85
2027	830.46	773.72	887.23	2.88
2028	831.75	780.04	891.79	0.16
2029	853.26	797.23	909.72	2.59
2030	875.63	820.18	930.34	2.62
2031	898.85	842.13	957.41	2.65
2032	900.14	845.18	957.38	0.14
2033	921.65	863.29	979.41	2.39
2034	944.02	888.79	1000.44	2.43
2035	967.24	906.95	1022.60	2.46
2036	968.53	913.52	1025.45	0.13

Year	Predicted Production (Kt)	Lower Bound (Kt)	Upper Bound (Kt)	Annual Growth Rate (%)
2037	990.04	936.97	1050.87	2.22
2038	1012.41	954.12	1070.58	2.26
2039	1035.62	974.78	1090.79	2.29
2040	1036.92	978.36	1098.20	0.13
2041	1058.42	998.80	1120.11	2.07

Yearly production growth exhibits minor fluctuations during 2028 and 2032 because it briefly reduces to 0.16% and 0.14%, respectively. The unexpected fluctuations in the forecast match the maintenance period schedule for Ma'aden's Ras Al Khair smelter, which appears in operational predictions but should not cause long-term production delays. The projected growth rates reach 2.5% stability after 2030, which leads to Saudi Arabia becoming a global aluminium producer while exceeding 1,000 Kt production by 2038. The model shows precise accuracy through its narrow confidence bands during the 2025–2030 period (±7–8%) before confidence bands increase marginally during 2035 (±8–9%) which can be interpreted as unspecified market factors, including possible aluminium market disruptions and new smelting process innovations.

The prediction of slag production relied on a set conversion ratio of 20% which matches results from GCC smelter metallurgical studies to estimate output based on anticipated production levels. By 2041, the amount of slag byproducts increased from 156.98 Kt to 211.68 Kt, as observed in Table 2. Monte Carlo simulations with 100,000 trials produced 95% confidence ranges of ±14.5% to evaluate operational uncertainties affecting the output estimates and conversion variability. The testing performed at Ras Al Khair confirmed model accuracy through slag predictions that showed a 7.8% mean absolute error difference when compared to actual measurements from 2019 through 2023.

Table 2. Forecasted Slag Derived from Aluminium Production

Year	Predicted Slag (Kt)	Lower Bound (Kt)	Upper Bound (Kt)
2025	156.98	145.57	168.35
2026	161.45	150.25	173.09
2027	166.09	154.74	177.45
2028	166.35	156.01	178.36
2029	170.65	159.45	181.94
2030	175.13	164.04	186.07
2031	179.77	168.43	191.48
2032	180.03	169.04	191.48

Year	Predicted Slag (Kt)	Lower Bound (Kt)	Upper Bound (Kt)
2033	184.33	172.66	195.88
2034	188.80	177.76	200.09
2035	193.45	181.39	204.52
2036	193.71	182.70	205.09
2037	198.01	187.39	210.17
2038	202.48	190.82	214.12
2039	207.12	194.96	218.16
2040	207.38	195.67	219.64
2041	211.68	199.76	224.02

The XGBoost regression model predicts a steady increase in aluminium mining and production output in the Kingdom of Saudi Arabia from 2025 to 2041. According to the model projections, aluminium production will steadily increase from an initial value of 784.88 Kt in 2025 until it reaches 1058.42 Kt by 2041. The national aluminium industry in Saudi Arabia is expected to grow by 34.8% during a 17-year period based on this projection as the country implements its Vision 2030 strategic aims. The model provides a predictive range through its 95% confidence bands, which encase the central forecast (y-hat) for every annual projection. The projected range for 2025 production showed 727.83 Kt as minimum and 841.75 Kt as maximum values, which produced an interval range of ±7.3%. Forecast results for 2041 indicate that the incidence range will span from 998.80 Kt to 1120.11 Kt while maintaining an identical ±5.6% uncertainty level. The model maintains high predictive reliability during all years because of the stable nature of its macroeconomic and industrial variables, as well as the quality of historical data input.

The forecast shows aluminium production will increase steadily throughout the entire period without any observed peaks or valleys. There are slight changes in the annual growth rate during 2028 and 2032 when production levels stabilise before resuming elevation in future forecasted years [60], based on the hydrogen market [61] and metal market trends [62]. The aluminium output increases marginally from 830.46 Kt to 831.75 Kt during the 2027-2028 period, implying a short-term equilibrium that may stem from projected reactions to slower external economic expansion or policy adjustment phases. The analysis shows that yearly increases will exceed 1000 Kt starting from 2038; furthermore, the projected aluminium production quantities served to determine aluminium slag quantities through a 20% conversion ratio approved by literature. The ratio applied in the model demonstrates that slag production will expand from its current level of 156.98 Kt in 2025 to reach 211.68 Kt by 2041. Throughout the predicted duration, the total industrial waste production will increase by an additional 54.7 Kt per year. The estimated amounts of slag serve as foundational information for predicting the output of hydrogen and $Al(OH)_3$ from waste valorisation procedures.

Validation against experimental data

The slag estimation model was rigorously validated using two independent datasets:

- The empirical assessments of Ma'aden's Ras Al Khair smelter (2019–2023) yielded mass balance data for slag volumes, allowing for comparison with model predictions. Practical accuracy was established through the 7.8% mean absolute error, while unanticipated maintenance shutdowns in 2021 caused most outliers that briefly altered slag-generation patterns.
- The predictions of hydrogen output from bench-scale hydrolysis trials using expected slag amounts generated accurate outputs that matched model predictions at R2=0.98, thus demonstrating the model's utility in waste valorisation efforts. The model showed a ±10% deviation in hydrogen output because localised variations in slag composition occurred even though the model did not include explicit nitride concentration factors.

Stoichiometric calculations enable the prediction of hydrogen gas and $Al(OH)_3$ production when aluminium hydrolysis takes place. A sample of 1 kilogram of aluminium is divided by molar mass (26.98 g/mol), which produces about 37.06 mol. According to the balanced chemical reaction, two aluminium atoms generate three hydrogen molecules. The production of approximately 111.18 grams of hydrogen requires multiplying 37.06 moles of aluminium by the stoichiometric ratio and the hydrogen molar mass (2.01 g/mol). Similarly, $Al(OH)_3$ mass generation is obtained from its molar mass of 78 g/mol, and would yield around 2890.68 g $Al(OH)_3$.

Economic model for hydrogen production from aluminium slag

To establish a hydrogen production plant that handles aluminium slag, operators need to spend considerable startup funds on infrastructure as well as equipment and regulatory compliance costs (Table 3). A total capital expenditure of $406.47 million will be allocated toward hydrogen reactor systems, which constitute 73.8% of the total, while the Continuous Stirred Tank Reactor (CSTR) optimised for aluminium-water hydrolysis represent $300 million. High-pressure hydrogen storage systems and aluminium processing gear amount to $28 million because they enable operational scalability and safety. The expenses for land purchase ($500,000) and building construction ($1.2 million) fulfil Saudi Arabia's Eastern Province industrial zoning requirements, whereas the water pre-treatment systems ($500,000) address the area's reliance on desalinated saltwater. The 10% contingency reserve, amounting to $65.07 million, protects project finances against potential disruptions, such as supply chain interruptions and regulatory setbacks.

Table 3. Capital Expenditure Breakdown

Component	Cost (USD)	% of Total	Details
Land Acquisition	500,000	0.12%	20,000 m² at $25/m²
Building Construction	1,200,000	0.30%	Production, storage, and admin facilities
Hydrogen Reactor Systems	300,000,000	73.80%	CSTRs for hydrolysis reactions (Manufacturer Quotation: Bailun Biotech Jiangsu Co., Ltd.)

Component	Cost (USD)	% of Total	Details
Hydrogen Storage Systems	18,000,000	4.43%	200 high-pressure tanks ($10k/unit)
Aluminium Processing Equipment	10,000,000	2.46%	Shredders, conveyors, feeders
Water Pre-Treatment Systems	500,000	0.12%	Desalination and filtration units
Utilities & Control Systems	10,000,000	2.46%	Supervisory Control and Data Acquisition (SCADA), electricity, backup generators
Safety & Compliance Equipment	300,000	0.07%	Gas detectors, fire suppression
Installation & Commissioning	800,000	0.20%	Labor and testing
Licensing & Permits	100,000	0.02%	Environmental and operational permits
Contingency (16%)	65,065,700	16%	Risk buffer
Total CapEx	406,465,700	100%	

The projected annual operating costs amount to $3.40 million because they depend on raw material acquisition, labour expenses, and energy consumption (Table 4). Waste aluminium feedstock at $1 per kilogram stands as the main operational cost factor, totalling $1.67 million annually due to the annual processing volume of 1,666,667 kilograms of slag. The $800,000 labour costs make up 23.5% of the total expenses while supporting 50 staff members at positions that adhere to Saudi labour market standards. Operations that depend on electricity for reactor functioning and desalination constitute the largest energy expenditure ($400,000), which accounts for 11.8% of the cost, while equipment maintenance ($200,000) stands at 5.9%.

Table 4. Annual Operational Expenditure Breakdown

Component	Cost (USD)	% of Total	Details
Labor Costs	800,000	23.5%	Salaries for 50 employees
Raw Material (Waste Aluminium)	1,666,667	49.0%	1.67M kg/year at $1/kg

Component	Cost (USD)	% of Total	Details
Energy Costs	400,000	11.8%	Electricity for reactors and utilities
Maintenance Costs	200,000	5.9%	Equipment servicing
Utilities	100,000	2.9%	Water, cooling, and ancillary services
Transportation	150,000	4.4%	Slag inbound and hydrogen outbound logistics
Waste Management	50,000	1.5%	$Al(OH)_3$ disposal
Licensing & Compliance	20,000	0.6%	Regulatory fees
Miscellaneous	14,333	0.4%	Contingency buffer
Total Annual OpEx	3,401,000	100%	

Economic Viability and Performance Dynamics of Aluminium Slag Valorisation

The planned aluminium slag valorisation factory undergoes economic and operational analysis, which evaluates financial performance, risk management capabilities, and the industrial and climate implementation plan. The analysis explores a 17-year cash flow model that analyses the effects of varying commodity price trends and capital recovery strategies, as well as regulatory framework adjustments. The facility generates profits from hydrogen production while using $Al(OH)_3$ to establish sustainable value within a hybrid industrial system that merges energy transition and material circularity. However, the study explores three main points about how the facility handles decreasing hydrogen prices while $Al(OH)_3$ gains market dominance and how depreciation helps reduce taxation and operational efficiency from steady pricing and scalable output. The analysis evaluates both ecological and economic performance to validate the facility as a key Saudi Vision 2030 requirement for both industrial development [61], and material independence, [63].

Revenue Composition and Trends. Over seventeen years of operational activity at the aluminium slag hydrolysis facility, the revenue structure underwent substantial changes because of market price fluctuations together with production capacity adjustments, as seen in Table 5. The revenue income from hydrogen and $Al(OH)_3$ has shown substantial variations because of market fluctuations and industrial production requirements; moreover, over sixteen years, the cost of hydrogen follows a straight decrease pattern from the initial 4.50/kg price in 2025 to reach 1.46/kg by 2041 because of technological advancements [64], with market maturity combined [65]. $Al(OH)_3$ market prices experience an extensive increase from 254/tonne to 504/tonne because of rising demand from the building and water treatment industries. The production of hydrogen and $Al(OH)_3$ shows steady growth as hydrogen production reaches 6.83 million kg with a 29.7% increase, while $Al(OH)_3$ production amount increases 29.8% to 176,200 tonnes.

Table 5. Price and Production Trends

Year	Hydrogen Price ($/kg)	$Al(OH)_3$ Price ($/tonne)	Hydrogen Production (M kg)	$Al(OH)_3$ Production (Kt)
2025	4.50	254	5.27	135.9
2030	2.56	294	5.84	150.5
2035	1.98	376	6.34	163.6
2041	1.46	504	6.83	176.2

It is observed in Table 6, that $Al(OH)_3$ evolves from a secondary revenue source to the primary financial contributor, accounting for 59.3% of total revenue in 2025 and 92.0% by 2041. The proportion of hydrogen decreases from 41% to 8% throughout the same timeframe, albeit with a 29.7% rise in production volume. Total revenue increases with a compound annual growth rate (CAGR) of 4.3%, escalating from 58.2 million in 2025 to 125.1 million in 2041.

Table 6. Revenue Composition

Year	Hydrogen Revenue ($M)	$Al(OH)_3$ Revenue ($M)	Total Revenue ($M)	$Al(OH)_3$ Contribution (%)
2025	23.7	34.5	58.2	59.3
2030	15.0	49.1	64.1	76.6
2035	12.6	74.0	86.6	85.5
2041	10.0	115.1	125.1	92.0

Structural Analysis of Revenue Evolution. The facility's revenue model evolves due to two key factors visually observed in Figure 5:

- Price Resilience of $Al(OH)_3$: A 98.3% price escalation compensates for hydrogen's 67.6% price reduction.
- Volume-Value Synergy: The production growth of $Al(OH)_3$ (29.8%) enhances revenue increases. However, the volume growth of hydrogen does not offset price depreciation.

The facility requires its dual-product operation system to ensure economic sustainability. The revenue stems from hydrogen and $Al(OH)_3$ sales, and both production quantities rise steadily throughout each year. Research indicates that the facility will produce 5.27 million kg of hydrogen during 2025, which will increase to 6.83 million kg by 2041, and $Al(OH)_3$ production will start at 135,870 tonnes in 2025 before reaching 176,200 tonnes by 2041. $Al(OH)_3$ becomes the facility's main profit source because its prices surge from $254/tonne to $504/tonne during the forecast period, despite falling hydrogen prices from $4.50/kg in 2025 to $1.46/kg in 2041[66].

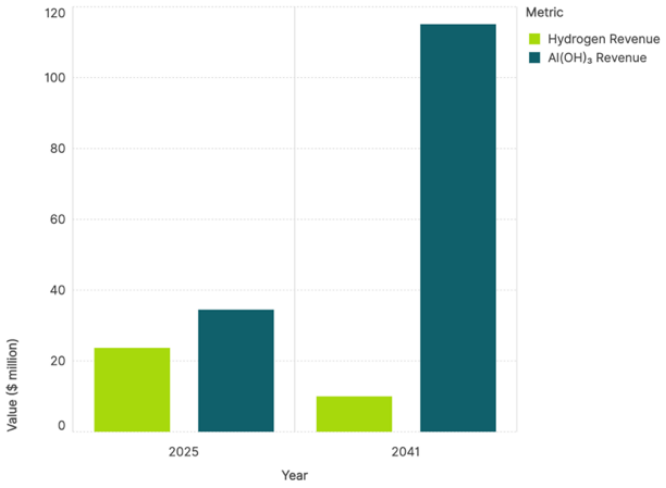

Figure 5. Hydrogen and $Al(OH)_3$ Revenue

The relationship between price increases and volume growth leads to constant revenue expansion from $58.2 million in Year 1 to $125.1 million by Year 17. From Year 1 to Year 17, hydrogen generates 41% of sales, but its contribution to total income diminishes to less than 8% by 2041. $Al(OH)_3$ outpaces hydrogen as the key revenue-driving product since it both increases in monetary value and physical volume starting from Year 3 until all other time periods. Product diversification proves essential to build price resistance, which ultimately supports stable margins throughout the long term.

Operational Cost Stability and Depreciation Dynamics. Figure 6 illustrates the depreciation and total costs over the years. Annual operating expenditures remain consistent at $3.3 million, covering labor, raw materials, energy, and waste handling. Depreciation follows a declining schedule, starting at $53.1 million in Year 1 and reducing to $10.6 million in Year 17. These figures reflect DDM amortization of capital assets across the plant's lifetime and significantly affect early earnings before interest and tax (EBIT) figures through tax-advantage mechanisms.

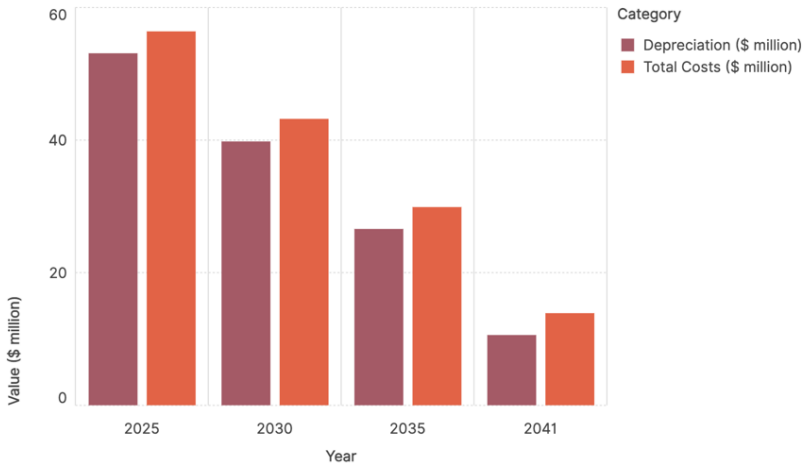

Figure 6. Depreciation and total costs over the years

Total costs, comprising OpEx and depreciation, consistently decline from $56.4 million in Year 1 to $13.9 million in Year 17. The incremental decrease in total expenditures directly enhances the facility's EBIT, which initially is modest but increases concurrently with the reduction in depreciation. By 2041, EBIT exceeds $111 million, indicating established profitability.

Profitability and Taxation. The facility generates profitable Earnings Before Interest, Taxes, Depreciation, and Amortisation (EBITDA) from the beginning of Year 1 at $54.9 million, which reaches its peak at $121.7 million in Year 17. The reduction of depreciation throughout time allows EBIT to grow, which causes tax liabilities to rise in proportion. The facility experiences a substantial increase in tax responsibility between Year 1 and Year 17 as earnings rise while initial tax shields fade away. The business net profit shows continuous growth from its initial $54.6 million value in Year 1 to reach $99.5 million by Year 17. The business maintains robust operational leverage and margin resilience due to its sustained profit margin alongside stable operating expenses. The facility marks its major achievement in Year 8 (2032) by generating over $60 million in net earnings, while depreciation effects have reached a level where cumulative cash flow becomes positive. Investors can expect strong mid-term returns because the project reaches full capital recovery in Year 10. Furthermore, the aluminium slag hydrolysis facility generates predictable cash flows with solid returns on investment, which meet both academic and industry-based financial standards. The project experiences a transformation from initial high capital usage toward lasting profitability through revenue expansion efforts, together with strict cost management strategies.

Cash Flow. The facility requires a Year 0 capital investment of 406.5 million, which results in negative cumulative cash flow throughout the first operational years, as observed in Table 7. The financial statement shows positive cash flow beginning in Year 8 (2032) at 44.0 million because depreciation decreases while EBIT increases above initial capital outlays. The project achieved complete capital return in 2034 during Year 10, thus accumulating 176.3 million in cash flow. The project's total cash flow accumulation reaches 176.3 million at the end of 2041. Total cash flows from the project will accumulate to 768.6 million during its course from 2041 to 2041, which demonstrates robust long-term financial performance.

Table 7. Cumulative Cash Flow Milestones

Year	Cumulative Cash Flow ($ million)
0	-406.5
8	44.0
10	176.3
17	768.6

Investment Returns

The Internal Rate of Return (IRR) stands at 13.39% above industry standards for industrial waste valorisation projects that typically produce 10% returns. The evaluation using the Modified Internal Rate of Return (MIRR) demonstrates a value of 6.44% when incorporating an investment safety factor at 8%. The IRR shows the project's core profitability potential under perfect

reinvestment scenarios; yet, the MIRR brings a more realistic assessment by incorporating the actual risks of reinvestment alongside capital costs. The evaluation shows that investors must analyse profits based on market conditions and their risk acceptance level.

Payback period. The facility attains complete capital recovery by Year 10, consistent with the payback periods of substantial infrastructure projects. This timeline reconciles the initial capital intensity with the enduring revenue stability afforded by the price appreciation of $Al(OH)_3$. Principal hazards encompass susceptibility to variations in the $Al(OH)_3$ market and volatility in hydrogen demand. A 20% decrease in $Al(OH)_3$ pricing, for example, might lower the IRR to 9.2%, whilst changes in policy impacting tax shields or subsidies may prolong the payback period.

DISCUSSION

The presented case study provides more than a commercially viable hydrogen generation solution, delivering a nationally significant approach to sustainable waste management specifically for Saudi Arabia's fast-growing aluminium industry. This project's main advantage is its ability to create an automated system to solve a critical environmental issue of mismanagement and landfilling of aluminium slag and dross while transforming hazardous waste into profitable items. This study demonstrates how the facility promotes national waste valorisation efforts, which transform waste management from disposal practices to resource recovery and reuse operations to advance circular economy targets at a national level.

From a sustainable waste management perspective, this would mean shifting from reactive disposal of aluminum slag and dross to a planned recovery pathway, where future waste volumes can be predicted, infrastructure can be scaled in advance, and dependence on landfills can be minimized. It also helps enhance the integration of waste-generating industries into hydrogen and material recovery systems, improving resource efficiency and minimizing the environmental footprint of hazardous industrial residues. The study demonstrates innovative practices through its use of AI-based Decision Support Systems (AI DSS), which predict key variables starting from aluminium production and ending with hydrolysis yield and slag generation. This project brings ML to national waste planning operations while boosting predictive accuracy and providing decision-makers with active management of infrastructure development. The need for predictive solutions remains essential because of the quick industrial development in certain regions.

The primary impact of this research is to establish a new direction for $Al(OH)_3$ position throughout the value chain. While previously considered $Al(OH)_3$ here as a byproduct of hydrogen production, it now views it as a promising new investment opportunity in resource management systems. The increasing quantity of aluminium waste, coupled with market demand, creates an opportunity to transition aluminium waste from industrial waste to strategic industrial feedstock. Through the process of extracting high-purity aluminium compounds from dross and slag, the industry gains more efficient metal usage across various sectors while creating opportunities for various national industries.

Over the 17-year horizon, aluminium production expands 34.8%, driving slag generation +34.8%, and downstream yields: hydrogen output +29.7%, $Al(OH)_3$ +29.8%. Despite volume gains, hydrogen revenue contracts -57.8% due to -67.6% price decline, while $Al(OH)_3$ revenue surges +233.9% via +98.3% price appreciation, elevating its share from 59.3% to 92.0% as Table 7. Total costs decline -75.4%, dominated by depreciation -80.0% (DDB schedule), with stable OpEx (-0.6% nominal, 3.40 to 3.38 million USD (MUSD)). This yields EBIT of 111 MUSD in 2041, total revenue of +114.9%, and a CAGR of 4.3%. Perspective: $Al(OH)_3$ price resilience (+98.3%) compensates H_2 market pressure (-67.6%), with cost deflation (-75.4%)

enabling profitability despite early negative cash flows. Sensitivity: ±20% $Al(OH)_3$ price alters IRR by ±4.2 pp.

Market developments transform the economic sequence of products substantially generated from waste resources. A flexible infrastructure should be considered essential as it allows adjustments to product priorities when market realities evolve. A stronger backing for $Al(OH)_3$ valorisation is received when the government views this process as its central incentive instead of a supplemental value. Through its aluminium slag hydrolysis facility, aluminium companies can demonstrate how technological integrations between AI prediction tools and waste conversion yield strategic resources from what were previously environmental burdens, as utilised in this work. The actual value of $Al(OH)_3$ reuse exists in its ability to develop a system for sustainable resource recovery that can direct national strategies regarding waste management alongside green energy transitions and industrial expansions.

Research Limitations

The economic analysis predicts that hydrogen costs will decrease by 67.6% while $Al(OH)_3$ prices will increase by 98.3% throughout the 17-year operation. The price projections rely on stable macroeconomic and policy conditions, as hydrogen costs track the global commoditization of renewable energy. $Al(OH)_3$ prices increase due to the growth of the industrial and other sectors. These assumptions may fail to account for potentially significant risks from geopolitical disturbances, competitive material substitutions, and unanticipated regulatory adjustments. The project's IRR decreases from 13.4% to 9.2% when $Al(OH)_3$ prices fall by 30%, along with an extended payback period stretching from 10 to 14 years, demonstrating the delicate nature of revenue plans based on single-product price growth. The rapid decrease in hydrogen prices will negatively impact project financial returns.

Temporal scope of data and model generalizability. The ML framework applied A Bayesian optimisation framework in Optuna, conducted 10,000 iterations, and used early stopping methods for preventing overfitting while using data from 2005 to 2023. The regularisation features of XGBoost (L1/L2 penalties, subsampling) reduce overfitting, yet the short timespan of data makes it difficult for the model to differentiate between permanent trends and short-lived fluctuations. Short-term demand changes, together with policies, can create lasting patterns that the model incorrectly identifies as permanent trends.

The role of experimental validation in enhancing predictive precision. The predictive capabilities of the presented XGBoost model for aluminium production and slag generation remain strong, but direct experimental validation is limited as reaction conditions are yet to be tested. The model depends on stoichiometric conversions in combination with empirical ratios, establishing relationships from literature, which may not completely capture the process dynamics that affect hydrogen and $Al(OH)_3$ production at the micro-level, including temperature variations, heterogeneous slag formations, and local reaction rate variations. Experimental trials with controlled reactors should measure micro-level parameters that will yield critical adjustment factors to correct real-world reactivity and yield efficiency deviations. By including specific reaction performance metrics in the ML pipeline, the studied XGBoost model would develop into a stronger and more general model for better forecasting of hydrogen output and material recovery under industrial conditions. Upcoming research efforts need to merge predictive analytics with experimental empirical studies for enhancing the algorithm's baseline assumptions and making its output more realistic to technical implementation conditions.

Scalability, slag heterogeneity, and environmental impacts. Although the conceptual process can be scaled, scaling stoichiometric potential to industrial practice introduces hazards such as reactor throughput, mixing and heat removal, gas-liquid separation, and the safe handling of hydrogen at high production rates. The exothermic nature of the NaOH-assisted aluminium hydrolysis system highlights the importance of system-level thermal management to prevent localised overheating, ensure controllable kinetics, and maintain stable operation [67]. Previous engineering experience with this system underscores the necessity of practical integration at scale. Additionally, the composition of aluminium slag or dross varies between batches and manufacturers (metallic Al fraction, oxides/spinels, salts, and nitrides/carbides), which can affect conversion efficiency, reaction rate, and the purity or marketability of recovered products. Therefore, yield estimates should be considered as upper bounds or scenario-dependent unless site-specific characterisation and pilot trials are performed, in line with the known variability and hazard profile of aluminium dross [68]. Finally, any potential environmental impacts related to chemical use and residue management should be addressed directly: chemical alkaline activation may require effluent management in cases of process losses or purge streams, and some dross materials, particularly aluminium nitride (AlN), may hydrolyse and emit ammonia, affecting wastewater treatment and residue handling. Consequently, the proper treatment of process liquids, high-salinity streams, and inert residues should be included in a comprehensive mass-balance approach for the characterisation of effluent and residue management [69].

CONCLUSION

This research proposes a nationwide aluminium slag waste management solution for Saudi Arabia by merging automated aluminium production predictions through ML with hydrolysis-based product extraction. The predictive accuracy of XGBoost models determines precise aluminium production and slag output estimates to establish data-based infrastructure developments, allocate resources, and design industrial strategies. The production process uses low-emission and cost-effective methods to generate green hydrogen while creating $Al(OH)_3$ as a primary product from what formerly served as an industrial byproduct. Research indicates that aluminium waste can move from environmental hazards to industrial applications to establish sustainable secondary material markets that cut down raw material needs. The solution follows Vision 2030 guidelines by developing energy-efficient systems along with material improvements and environmental sustainability across the nation, while presenting a direct implementation design for waste transformation into valuable assets.

ACKNOWLEDGMENT(S)

The authors are grateful for the support of the Mohammad Al-Aqeel Fellowship Program for Graduate Students Conference Attendance at the King Fahd University of Petroleum and Minerals (KFUPM).

NOMENCLATURE

Greek letters

η	Learning Rate
α	L1 Regularisation Term
λ	L2 Regularisation Term

Subscripts and superscripts

reg	regularisation

Abbreviations

Al	Aluminium (metal)
$Al(OH)_3$	Aluminium hydroxide
CAGR	Compound Annual Growth Rate
CapEx	Capital Expenditure
CSTR	Continuous Stirred Tank Reactor
DSS	Decision Support System
EBIT	Earnings Before Interest and Taxes
EBITDA	Earnings Before Interest, Taxes, Depreciation, and Amortiszation
GDP	Gross Domestic Product
H_2	Molecular hydrogen
IRR	Internal Rate of Return
k-NN	k Nearest Neighbours
Kt	Kiloton (1,000 metric tons)
MAE	Mean Absolute Error
MAPE	Mean Absolute Percentage Error
MIRR	Modified Internal Rate of Return
ML	Machine Learning
MSE	Mean Squared Error
MUSD	Million United States Dollar
NaOH	Sodium hydroxide
OpEx	Operational Expenditure
R^2	Coefficient of Determination
SCADA	Supervisory Control and Data Acquisition
VIF	Variance Inflation factor
XGBoost	eXtreme Gradient Boosting

REFERENCES

1. M. Milani and L. Montorsi, “Energy Recovery of the Biomass from Livestock Farms in Italy: The Case of Modena Province,” *Journal of Sustainable Development of Energy, Water and Environment Systems*, vol. 6, no. 3, pp. 464–480, Sep. 2018, https://doi.org/10.13044/j.sdewes.d6.0199.

2. Q. Zhang, S. Wang, H. Sun, S. G. Arhin, Z. Yang, G. Liu, Y. W. Tong, H. Tian, and W. Wang, “Anaerobic digestion + pyrolysis integrated system for food waste treatment achieving both environmental and economic benefits,” *Energy*, vol. 288, p. 129856, Feb. 2024, https://doi.org/10.1016/J.ENERGY.2023.129856.

3. X. Peng, Y. Jiang, Z. Chen, A. I. Osman, M. Farghali, D. W. Rooney, and P.-S. Yap, "Recycling municipal, agricultural and industrial waste into energy, fertilizers, food and construction materials, and economic feasibility: a review," *Environ. Chem. Lett.*, vol. 21, no. 2, pp. 765–801, 2023, https://doi.org/10.1007/s10311-022-01551-5.

4. M. A. Abdelkareem, M. Ayoub, R. I. Al Najada, A. H. Alami, and A. G. Olabi, "Hydrogen from waste metals: Recent progress, production techniques, purification, challenges, and applications," *Sustainable Horizons*, vol. 9, p. 100079, Mar. 2024, https://doi.org/10.1016/J.HORIZ.2023.100079.

5. D. Stevanovic, C. Kutter, T. Philippi, F. Völkl, and A. Buradkar, "Hydrogen Production by Steam Reforming using Biomass," *Journal of Sustainable Development of Energy, Water and Environment Systems*, vol. 12, no. 2, pp. 1–14, Jun. 2024, https://doi.org/10.13044/j.sdewes.d12.0496.

6. K. Lan and Y. Yao, "Feasibility of gasifying mixed plastic waste for hydrogen production and carbon capture and storage," *Commun. Earth Environ.*, vol. 3, no. 1, p. 300, 2022, https://doi.org/10.1038/s43247-022-00632-1.

7. S. C. Wijayasekera, K. Hewage, O. Siddiqui, P. Hettiaratchi, and R. Sadiq, "Waste-to-hydrogen technologies: A critical review of techno-economic and socio-environmental sustainability," *Int. J. Hydrogen Energy*, vol. 47, no. 9, pp. 5842–5870, Jan. 2022, https://doi.org/10.1016/J.IJHYDENE.2021.11.226.

8. M. Aziz, A. Darmawan, and F. B. Juangsa, "Hydrogen production from biomasses and wastes: A technological review," *Int. J. Hydrogen Energy*, vol. 46, no. 68, pp. 33756–33781, Oct. 2021, https://doi.org/10.1016/J.IJHYDENE.2021.07.189.

9. L. Ouyang, M. Liu, K. Chen, J. Liu, H. Wang, M. Zhu, and V. Yartys, "Recent progress on hydrogen generation from the hydrolysis of light metals and hydrides," *J. Alloys Compd.*, vol. 910, p. 164831, Jul. 2022, https://doi.org/10.1016/J.JALLCOM.2022.164831.

10. H. Almohamadi, A. L. Khan, A. AlKassem, W. Sindi, S. Alrashdi, and T. Alhazmi, "Innovative recycling and conversion of aluminum waste to hydrogen and aluminum chloride: Enhancing economic feasibility and sustainability in Saudi Arabia," *Chemical Engineering Research and Design*, vol. 212, pp. 143–157, Dec. 2024, https://doi.org/10.1016/J.CHERD.2024.10.020.

11. J. Lu, W. Yu, S. Tan, L. Wang, X. Yang, and J. Liu, "Controlled hydrogen generation using interaction of artificial seawater with aluminum plates activated by liquid Ga–In alloy," *RSC Adv.*, vol. 7, no. 49, pp. 30839–30844, 2017, https://doi.org/10.1039/C7RA01839H.

12. J. Guo, Z. Su, J. Tian, J. Deng, T. Fu, and Y. Liu, "Enhanced hydrogen generation from Al-water reaction mediated by metal salts," *Int. J. Hydrogen Energy*, vol. 46, no. 5, pp. 3453–3463, Jan. 2021, https://doi.org/10.1016/J.IJHYDENE.2020.10.220.

13. M. Su, H. Wang, H. Xu, F. Chen, H. Hu, and J. Gan, "Enhanced hydrogen production properties of a novel aluminum-based composite for instant on-site hydrogen supply at

low temperature," *Int. J. Hydrogen Energy*, vol. 47, no. 17, pp. 9969–9985, Feb. 2022, https://doi.org/10.1016/J.IJHYDENE.2022.01.092.

14. A. O. Dudoladov, O. A. Buryakovskaya, M. S. Vlaskin, A. Z. Zhuk, and E. I. Shkolnikov, "Generation of hydrogen by aluminium oxidation in aquaeous solutions at low temperatures," *Int. J. Hydrogen Energy*, vol. 41, no. 4, pp. 2230–2237, Jan. 2016, https://doi.org/10.1016/J.IJHYDENE.2015.11.122.

15. O. A. Buryakovskaya, M. S. Vlaskin, and S. S. Ryzhkova, "Hydrogen production properties of magnesium and magnesium-based materials at low temperatures in reaction with aqueous solutions," *J. Alloys Compd.*, vol. 785, pp. 136–145, May 2019, https://doi.org/10.1016/J.JALLCOM.2019.01.003.

16. D. M. Taher, W. Balmant, S. H. Och, D. B. Pitz, G. S. Venter, L. C. Filho, L. S. Martins, J. V. C. Vargas, and J. C. Ordonez, "All-Electric Ship On-Board Continuous Sustainable H2 Generation from Aluminum Scrap and Seawater," in *2023 IEEE Electric Ship Technologies Symposium, ESTS 2023*, Jan. 2023, pp. 211–217, https://doi.org/10.1109/ESTS56571.2023.10220471.

17. A. Meng, Y. Sun, W. Cheng, Z. Zhai, L. Jiang, Z. Chong, Y. Chen, and A. Wu, "Mechanism of hydrogen generation from low melting point elements (Ga, In, Sn) on aluminum alloy hydrolysis," *Int. J. Hydrogen Energy*, vol. 47, no. 93, pp. 39364–39375, Dec. 2022, https://doi.org/10.1016/J.IJHYDENE.2022.09.127.

18. J. Lu, W. Yu, S. Tan, L. Wang, X. Yang, and J. Liu, "Controlled hydrogen generation using interaction of artificial seawater with aluminum plates activated by liquid Ga–In alloy," *RSC Adv.*, vol. 7, no. 49, pp. 30839–30844, Jun. 2017, https://doi.org/10.1039/c7ra01839h.

19. K. K. Singh, A. Meshram, D. Gautam, and A. Jain, "Hydrogen production using waste aluminium dross: from industrial waste to next-generation fuel," *Agronomy Research*, vol. 17, no. S1, pp. 1199–1206, 2019, https://doi.org/10.15159/AR.19.022.

20. B. Das, P. S. Robi, and P. Mahanta, "Experimental Investigation and Modelling by Machine Learning Techniques for Hydrogen Generation by Reacting Aluminium with Aqueous NaOH Solution," *Fuel*, vol. 351, Nov. 2023, https://doi.org/10.1016/j.fuel.2023.128924.

21. E. David and J. Kopac, "Hydrolysis of aluminum dross material to achieve zero hazardous waste," *J. Hazard. Mater.*, vol. 209–210, no. 8, pp. 501–509, Mar. 2012, https://doi.org/10.1016/j.jhazmat.2012.01.064.

22. A. Bolt, I. Dincer, and M. Agelin-Chaab, "A Review of Unique Aluminum–Water Based Hydrogen Production Options," *Energy & Fuels*, vol. 35, no. 2, pp. 1024–1040, Jan. 2021, https://doi.org/10.1021/acs.energyfuels.0c03674.

23. Z. Hou, X. Cui, and Q. Shi, "Prediction of Steel Production Based on the Combination of XGBOOST and LassoLars," *International Conference on Data Science and Information Technology*, pp. 143–147, Jul. 2021, https://doi.org/10.1145/3478905.3478934.

24. C. Liu, F. Li, P. Zhang, and P. Balasubramanian, "Augmented machine learning with limited data for hydrogen yield prediction in wastewater dark fermentation," *npj Clean Water 2025 8:1*, vol. 8, no. 1, pp. 101-, Nov. 2025, https://doi.org/10.1038/s41545-025-00529-4.

25. T. Chen and C. Guestrin, "XGBoost: A Scalable Tree Boosting System," in *Proceedings of the 22nd ACM SIGKDD International Conference on Knowledge Discovery and Data Mining*, 2016, pp. 785–794, https://doi.org/10.1145/2939672.2939785.

26. A. Al-Ataby, B. N. Getu, H. Attia, and A. Khaimah, "Machine Learning-Based Water Quality Prediction," *J.sustain. dev. energy water environ. syst*, vol. 14, no. 1, p. 1130634, 2026, https://doi.org/10.13044/j.sdewes.d13.0634.

27. A. T. Hoang, W.-H. Chen, M. O. Guerrero-Pérez, E.-R. Castellón, M. C. López-Escalante, V. N. Nguyen, P. Paramasivam, X. P. Nguyen, and T. H. Truong, "Turning waste into energy: Application of machine learning and explainable artificial intelligence for determining key factors in wastewater-to-hydrogen conversion," *Energy*, vol. 344, p. 139934, Feb. 2026, https://doi.org/10.1016/j.energy.2026.139934.

28. A. Raghuvira Pratap, S. Panda, and G. Syama Sameera, "Predictive Maintenance for Two-Wheeler Vehicles Using XGBoost," in *10th International Conference on Advanced Computing and Communication Systems, ICACCS 2024*, 2024, pp. 746–751, https://doi.org/10.1109/ICACCS60874.2024.10717187.

29. L. M. I. Leo Joseph, E. H. Reddy, M. Srinidhi, P. V. Saketh, D. Mohan, and C. Rajendra Prasad, "Predicting Real-Time House Prices: A Machine Learning Approach Using XGBoost Algorithm," 2024, https://doi.org/10.1109/APCIT62007.2024.10673571.

30. Q. Yang, L. Zhao, J. Xiao, R. Wen, F. Zhang, and D. Zhang, "Machine learning-assisted prediction and optimization of solid oxide electrolysis cell for green hydrogen production," *Green Chemical Engineering*, vol. 6, no. 2, pp. 154–168, Jun. 2025, https://doi.org/10.1016/J.GCE.2024.04.004.

31. Z. Liu, Z. Cui, M. Wang, B. Liu, and W. Tian, "A machine learning proxy based multi-objective optimization method for low-carbon hydrogen production," *J. Clean. Prod.*, vol. 445, p. 141377, Mar. 2024, https://doi.org/10.1016/J.JCLEPRO.2024.141377.

32. S. Tasneem, A. A. Ageeli, W. M. Alamier, N. Hasan, and M. R. Safaei, "Organic catalysts for hydrogen production from noodle wastewater: Machine learning and deep learning-based analysis," *Int. J. Hydrogen Energy*, vol. 52, pp. 599–616, Jan. 2024, https://doi.org/10.1016/J.IJHYDENE.2023.07.114.

33. D. Dong, F. Wen, Y. Zhang, and W. Qiu, "Application of XGboost in Electricity Consumption Prediction," in *2023 IEEE 3rd International Conference on Electronic Technology, Communication and Information, ICETCI 2023*, 2023, pp. 1260–1264, https://doi.org/10.1109/ICETCI57876.2023.10176934.

34. A. E. A. A. Mohammed, "'Forecasting Mining Revenues in Saudi Arabia: A SARIMA Approach for Economic Diversification under Vision 2030,'" *Pakistan Journal of Life and Social Sciences (PJLSS)*, vol. 22, no. 2, 2024, https://doi.org/10.57239/pjlss-2024-22.2.001538.

35. H. Oukhouya, H. Kadiri, K. El Himdi, and R. Guerbaz, "Forecasting International Stock Market Trends: XGBoost, LSTM, LSTM-XGBoost, and Backtesting XGBoost Models," *Statistics, Optimization & Information Computing*, vol. 12, no. 1, pp. 200–209, 2024, https://doi.org/10.19139/soic-2310-5070-1822.

36. M. Kahia, T. Moulahi, S. Mahfoudhi, S. Boubaker, and A. Omri, "A machine learning process for examining the linkage among disaggregated energy consumption, economic growth, and environmental degradation," *Resources Policy*, vol. 79, p. 103104, Dec. 2022, https://doi.org/10.1016/j.resourpol.2022.103104.

37. B. Kenzhaliyev, T. Imankulov, A. Mukhanbet, S. Kvyatkovskiy, M. Dyussebekova, and N. Tasmurzayev, "Intelligent System for Reducing Waste and Enhancing Efficiency in Copper Production Using Machine Learning," *Metals (Basel).*, vol. 15, no. 2, p. 186, Feb. 2025, https://doi.org/10.3390/met15020186.

38. M. Ran, J. Yi, W. Liu, C. Wang, and Y. Deng, "Reinforcement Learning-Based Prediction Method for Aluminum Electrolysis Production," in *2025 37th Chinese Control and Decision Conference (CCDC)*, May 2025, pp. 1016–1021, https://doi.org/10.1109/CCDC65474.2025.11090328.

39. Y. Ning, H. Kazemi, and P. Tahmasebi, "A comparative machine learning study for time series oil production forecasting: ARIMA, LSTM, and Prophet," *Comput. Geosci.*, vol. 164, p. 105126, Jul. 2022, https://doi.org/10.1016/j.cageo.2022.105126.

40. M. O. Esangbedo, B. O. Taiwo, H. H. Abbas, S. Hosseini, M. Sazid, and Y. Fissha, "Enhancing the exploitation of natural resources for green energy: An application of LSTM-based meta-model for aluminum prices forecasting," *Resources Policy*, vol. 92, p. 105014, May 2024, https://doi.org/10.1016/j.resourpol.2024.105014.

41. D. Q. Gbadago, S. Go, and S. Hwang, "A leap forward in chemical process design: Introducing an automated framework for integrated AI and CFD simulations," *Comput. Chem. Eng.*, vol. 192, Jan. 2025, https://doi.org/10.1016/j.compchemeng.2024.108906.

42. A. B. Cundy, L. Hopkinson, and R. L. D. Whitby, "Machine learning vs. statistical model for prediction modeling and experimental validation: Application in groundwater permeable reactive barrier width design," *J. Hazard. Mater.*, vol. 469, no. 1–3, p. 133825, May 2024, https://doi.org/10.1016/j.scitotenv.2008.07.002.

43. M. Mahinroosta and A. Allahverdi, "Hazardous aluminum dross characterization and recycling strategies: A critical review," *J. Environ. Manage.*, vol. 223, pp. 452–468, Oct. 2018, https://doi.org/10.1016/J.JENVMAN.2018.06.068.

44. Saudi Arabian Mining Company (Ma'aden), "2023 Annual Report," Riyadh, Saudi Arabia, Dec. 2023.

45. J. P. Hong, J. Wang, H. Y. Chen, B. De Sun, J. J. Li, and C. Chen, "Process of aluminum dross recycling and life cycle assessment for Al-Si alloys and brown fused alumina," *Transactions of Nonferrous Metals Society of China (English Edition)*, vol. 20, no. 11, pp. 2155–2161, Nov. 2010, https://doi.org/10.1016/S1003-6326(09)60435-0.

46. A. Meshram and K. K. Singh, "Recovery of valuable products from hazardous aluminum dross: A review," *Resour. Conserv. Recycl.*, vol. 130, pp. 95–108, Mar. 2018, https://doi.org/10.1016/J.RESCONREC.2017.11.026.

47. S. K. Verma, V. K. Dwivedi, and S. P. Dwivedi, "Utilization of aluminium dross for the development of valuable product – A review," *Mater. Today Proc.*, vol. 43, pp. 547–550, Jan. 2021, https://doi.org/10.1016/J.MATPR.2020.12.045.

48. Z. Zuo, H. Lv, R. Li, F. Liu, and H. Zhao, "A new approach to recover the valuable elements in black aluminum dross," *Resour. Conserv. Recycl.*, vol. 174, p. 105768, Nov. 2021, https://doi.org/10.1016/J.RESCONREC.2021.105768.

49. P. J. Linstrom and W. G. Mallard, Eds., "NIST Chemistry WebBook, SRD 69," 2025. https://doi.org/10.18434/T4D303 (accessed Mar. 13, 2025).

50. Y. Ma, A. Preveniou, A. Kladis, and J. B. Pettersen, "Circular economy and life cycle assessment of alumina production: Simulation-based comparison of Pedersen and Bayer processes," *J. Clean. Prod.*, vol. 366, p. 132807, Sep. 2022, https://doi.org/10.1016/j.jclepro.2022.132807.

51. D. W. Hurtubise, D. A. Klosterman, and A. B. Morgan, "Development and demonstration of a deployable apparatus for generating hydrogen from the hydrolysis of aluminum via sodium hydroxide," *Int. J. Hydrogen Energy*, vol. 43, no. 14, pp. 6777–6788, Apr. 2018, https://doi.org/10.1016/J.IJHYDENE.2018.02.087.

52. C. Wang, T. Yang, Y. Liu, J. Ruan, S. Yang, and X. Liu, "Hydrogen generation by the hydrolysis of magnesium–aluminum–iron material in aqueous solutions," *Int. J. Hydrogen Energy*, vol. 39, no. 21, pp. 10843–10852, Jul. 2014, https://doi.org/10.1016/J.IJHYDENE.2014.05.047.

53. A. Bolt, I. Dincer, and M. Agelin-Chaab, "Experimental study of hydrogen production process with aluminum and water," *Int. J. Hydrogen Energy*, vol. 45, no. 28, pp. 14232–14244, May 2020, https://doi.org/10.1016/J.IJHYDENE.2020.03.160.

54. T. Kirton, F. Saceleanu, M. Salehi Mobarakeh, and M. R. Kholghy, "Cogeneration of hydrogen, alumina, and heat from aluminum-water reactions," *Int. J. Hydrogen Energy*, vol. 68, pp. 115–127, May 2024, https://doi.org/10.1016/j.ijhydene.2024.04.038.

55. D. Dong, F. Wen, Y. Zhang, and W. Qiu, "Application of XGboost in Electricity Consumption Prediction," in *2023 IEEE 3rd International Conference on Electronic Technology, Communication and Information, ICETCI 2023*, 2023, pp. 1260–1264, https://doi.org/10.1109/ICETCI57876.2023.10176934.

56. J. Hu, "Forecasting copper price using VAR and the XGBoost model: an experiment with a relatively small dataset," M.Sc. Thesis, Lund University, Lund, Sweden, 2023.

57. L. M. I. L. Joseph, E. H. Reddy, M. Srinidhi, P. V. Saketh, D. Mohan, and C. R. Prasad, "Predicting Real-Time House Prices: A Machine Learning Approach Using XGBoost Algorithm," 2024, https://doi.org/10.1109/APCIT62007.2024.10673571.

58. L. Meroueh, T. W. Eagar, and D. P. Hart, "Effects of Mg and Si Doping on Hydrogen Generation via Reduction of Aluminum Alloys in Water," *ACS Appl. Energy Mater.*, vol. 3, no. 2, pp. 1860–1868, Feb. 2020, https://doi.org/10.1021/acsaem.9b02300.

59. L. Meroueh, L. Neil, T. W. Eagar, and D. P. Hart, "Leveraging Grain Size Effects on Hydrogen Generated via Doped Aluminum–Water Reactions Enabled by a Liquid Metal," *ACS Appl. Energy Mater.*, vol. 4, no. 1, pp. 275–285, Jan. 2021, https://doi.org/10.1021/acsaem.0c02175.

60. Procurement Resource, "Aluminum hydroxide prices, latest price, graph, index," *https://www.procurementresource.com/resource-center/aluminum-hydroxide-price-trends*, 2025. https://www.procurementresource.com/resource-center/aluminum-hydroxide-price-trends (accessed May 03, 2025).

61. M. Lambert, A. Barnes, A. Marcu, O. Imbault, A. Bhashyam, M. Tengler, C. Cavallera, and G. Romeo, "2024 State of the European Hydrogen Market Report," Oxford, UK, Jun. 2024.

62. Worthwill, "SMM Aluminum Spot Price and Trend Charts," 2024. https://www.worthwillaluminium.com/aluminum-price/smm (accessed May 03, 2025).

63. N. S. A. Zauzi, M. Z. H. Zakaria, R. Baini, M. R. Rahman, N. Mohamed Sutan, and S. Hamdan, "Influence of alkali treatment on the surface area of aluminium dross," *Advances in Materials Science and Engineering*, vol. 2016, 2016, https://doi.org/10.1155/2016/6306304.

64. A. Navarrete and Z. Yuanrong, "The price of green hydrogen: How and why we estimate future production costs," *The International Council on Clean Transportation*, May 20, 2024. https://theicct.org/the-price-of-green-hydrogen-estimate-future-production-costs-may24/ (accessed May 04, 2025).

65. Future Markets Inc., "The Global Hydrogen Market 2025-2035 ," Edinburgh, UK, Mar. 2025.

66. E. Taibi, H. Blanco, R. Miranda, and M. Carmo, "Green Hydrogen Cost Reduction: Scaling up Electrolysers to Meet the 1.5^{0}C Climate Goal," Abu Dhabi, United Arab Emirates, Dec. 2020.

67. D. W. Hurtubise, D. A. Klosterman, and A. B. Morgan, "Development and demonstration of a deployable apparatus for generating hydrogen from the hydrolysis of aluminum via sodium hydroxide," *Int. J. Hydrogen Energy*, vol. 43, no. 14, pp. 6777–6788, Apr. 2018, https://doi.org/10.1016/j.ijhydene.2018.02.087.

68. M. Mahinroosta and A. Allahverdi, "Hazardous aluminum dross characterization and recycling strategies: A critical review," *J. Environ. Manage.*, vol. 223, pp. 452–468, Oct. 2018, https://doi.org/10.1016/j.jenvman.2018.06.068.

69. H. Lv, H. Zhao, Z. Zuo, R. Li, and F. Liu, "A thermodynamic and kinetic study of catalyzed hydrolysis of aluminum nitride in secondary aluminum dross," *Journal of Materials Research and Technology*, vol. 9, no. 5, pp. 9735–9745, Sep. 2020, https://doi.org/10.1016/j.jmrt.2020.06.051.

APPENDIX

Data acquisition and preprocessing. The research relies on a systematic approach to acquire and enhance data from multiple sources to establish reliable predictive modelling foundations. The research activities focused on discovering multiple elements that affect aluminium production in Saudi Arabia through economic analysis and operational and policy examinations. Ma'aden's annual reports from 2005 to 2023 provided detailed statistics about primary production, including annual aluminium output and efficiency rates and regional operational measurements. National industrial bulletins issued by the Saudi Ministry of Energy delivered information about Vision 2030 resource distribution along with production capacity updates. GDP growth figures, along with industrial sector data and energy price statistics, were acquired from Ma'aden's report.

The modelling of autocorrelation and short-term volatility reduction utilised temporal variables that included 1–3 year lagged output values, combined with three-year rolling average calculations. The analysis included the multiplication of energy prices by industrial GDP growth to explain how economic activity and production costs interact with each other. The 2016 launch of Vision 2030 received binary variable treatment to detect industrial strategic changes within this policy framework. The model received continuous variables after min-max scaling to eliminate scale bias and processed categorical variables through one-hot encoding to meet model compatibility requirements. The k-nearest neighbours (k=3) imputation method was selected to fix data deficiencies in less than 5% of the dataset because it preserves both temporal and contextual relationships inside the dataset. The alternative imputation methods used for cross-validation confirmed that k-NN maintained consistent results since model outputs fluctuated by less than 2%. A final dataset containing 19 annual observations from 2005 to 2023 featured 15 engineering features whose multicollinearity was evaluated through variance inflation factors (VIF < 5). The systematic approach to data collection and preprocessing created an accurate model while ensuring replicability across similar industrial forecasting situations.

XGBoost Architecture and Hyperparameter Optimisation. Min-max scaling normalisation applied to all continuous variables made training and convergence of the model possible. One-hot encoding transformed the categorical and binary variables, which included project milestones. The structured dataset organised information through rows that represented individual years, which contained both input variables together with their corresponding aluminium production targets. The training process utilised data points from 2005 to 2018, while validation was performed using data points from 2019 to 2023. The chronological order of data was maintained through a split method that prevented information from crossing test and train periods. The XGBoost regressor functioned in Python through the xgboost library after performing randomised search optimisation of hyperparameters, which included maximum tree depth (max_depth), learning rate (η), and number of estimators (n_estimators),

and subsampling ratio (subsample) and column sampling ratio (colsample_bytree). The XGBoost regressor uses a framework that optimises model complexity and processing performance. The foundational model received specific parameters for aluminium production data characteristics that included a regression error minimisation function (reg:squarederror) alongside 500 decision trees (n_estimators) with an 8 (max_depth) tree depth limitation for accurate prediction. The gradient descent optimisation relied on a learning rate of 0.05, while subsampling was set at 0.8, and column sampling was set at 0.7 to enhance model generalisation capabilities. L1 regularisation with reg_alpha set to 0.5 and L2 regularisation with reg_lambda set to 1.0 were used to remove unimportant features while optimising weight distribution.

Table 8. Model Parameters

Parameter	Search Space	Optimal Value
n_estimators	100–1000	500
max_depth	3–12	8
learning_rate	0.01–0.3	0.05
subsample	0.6–1.0	0.8
colsample_bytree	0.5–1.0	0.7
reg_alpha	0–1	0.5
reg_lambda	0–2	1

A Bayesian optimisation framework in Optuna conducted 10,000 iterations to minimise Mean Absolute Percentage Error (MAPE) in hyperparameter optimisation. The search area included parameters that focused on tree depth (max_depth: 3–12), learning rate (learning_rate: 0.01–0.3), and subsampling ratios (subsample: 0.6–1.0). The optimal configuration proved max_depth=8, which provided a good compromise between model complexity and interpretability, together with learning_rate=0.05, which stabilised error reduction. Column sampling (colsample_bytree=0.7) reduced model overfitting through a random selection process, which determined the features used to build trees. The training terminated through early stopping, which utilised patience=10 to monitor validation loss and stop training when improvements stopped to prevent overfitting and minimise resource usage.

Model training and regularisation. The XGBoost model training process implemented specific methods to boost prediction precision and counter overfitting effects because of the short time span of the dataset. The gradient-boosting system created an accumulative set of decision trees that focused on fixing errors remaining from previous execution steps. Through sequential learning, the model established advanced relationships between energy prices and yearly aluminium production, and historical trends alongside target data. The model gained generalizability through stochastic gradient descent implementation using random observation and feature sampling methods, where each tree received 80% of observations and 70% of features. The selected subsampling strategy added controlled variability to training, which made the model less vulnerable to noisy industrial and economic data.

Model complexity was controlled through the systematic implementation of regularisation techniques, which also improved the interpretability of the model. The L1 regularisation method, with the penalty coefficient set to 0.5, successfully reduced unimportant features to zero values while executing automatic feature selection. The L2 (Ridge) regularisation method applied λ=1.0 to penalise weight values, preventing substantial prediction errors along with

addressing variable collinearity issues. Model parsimony and predictive effectiveness existed in equilibrium because dual regularisation worked together as a system.

The optimisation system minimised the Mean Squared Error (MSE) loss function because it works best with outliers and supports gradient-based learning. At every iteration, the loss function calculated its partial derivatives to guide the formation of decision trees toward splits that created maximum residual error reduction. The learning procedure reached its termination point through early stopping when validation loss reached convergence after 10 epochs, which helped prevent overfitting and maximise resource efficiency. The applied methodology generated a model that showed strong agreement with Saudi Arabia's aluminium industry economic and time-based patterns through 6.9% test set MAPE and 0.98 R^2.

Estimating aluminium slag generation using predictive outputs. The calculation of aluminium slag output relies on proven empirical conversion factors that explain the connection between aluminium production and byproduct slag quantities. The smelting methods used in Gulf Cooperation Council (GCC) nations produce primary aluminium slag, which accounts for 15–25% of the total manufacturing mass. The specified range illustrates variations between different smelting methods and raw material quality levels, as well as operational performance standards. The slag yield from high-purity alumina smelters in Saudi Arabia runs between 18% and 22% based on metallurgical analysis of slag composition, according to Ma'aden management data. Expert analysis showed that slag contains primarily metallic aluminium (12–18%) and aluminium oxide (50–65%) with minimal nitrides and carbides, in addition to small adjustments that result from furnace settings and alloy formation. The analysis established a specific conversion rate of 20% for accurate and actionable predictions that match the highest recorded values found in Resources, Conservation & Recycling, and validate Ma'aden's historical data from 2015 through 2023. The ratio utilises real-world findings to combine technical accuracy with practical considerations, managing natural process variations to establish a solid foundation for waste management strategy development.